

ARTICLES

Dielectric Relaxation of Concentrated Alkaline Aluminate Solutions

Richard Buchner,^{*,†} Pál Sipos,[‡] Glenn Hefter,^{*} and Peter M. May

Chemistry - DSE, Murdoch University, Murdoch, W.A. 6150, Australia

Received: November 29, 2001; In Final Form: May 3, 2002

The complex dielectric permittivity of concentrated aqueous alkaline aluminate solutions at total concentrations $1 \lesssim [\text{Al}]_{\text{T}}/\text{mol dm}^{-3} \lesssim 6$ with either $[\text{Na}]_{\text{T}} = 8.33 \text{ mol dm}^{-3}$ or $[\text{Al}]_{\text{T}}/[\text{Na}]_{\text{T}} = 0.750$ has been determined at 25 °C in the frequency range $0.5 \lesssim \nu/\text{GHz} \leq 20$. All solution spectra could be represented as a superposition of a Cole–Cole relaxation-time distribution for the solvent relaxation with an additional low-frequency Debye dispersion assigned to the solute. The variation of the effective hydration number, deduced from the water dispersion amplitude, shows that the aluminate ion, $\text{Al}(\text{OH})_4^-$, is less strongly solvated than the hydroxide ion, OH^- . Additionally, a “melting” of the hydration shells is observed at high concentration, probably due to co-sphere overlap and/or packing effects. The features of the solute relaxation are consistent with solvent-shared ion pairs of Na^+ with a previously proposed dimeric anion, $[(\text{HO})_3\text{Al}-\text{O}-\text{Al}(\text{OH})_3]^{2-}$. However, the data are not sufficient for an unequivocal assignment.

1. Introduction

Concentrated alkaline aluminate solutions are of great technological significance because they form the basis of the Bayer process, used for the recovery of purified $\text{Al}(\text{OH})_3$ from bauxitic ores. As in most technological processes, the industrial solutions, known as Bayer “liquors”, are complex mixtures of the desired species and a diversity of impurities and side products. For this reason, it is more fruitful to investigate the behavior of synthetic Bayer liquors, which contain only the species of interest. Such solutions exhibit many of the important characteristics of the industrial solutions, including the unusually slow kinetics of precipitation of $\text{Al}(\text{OH})_3$. Many of these features are thought to be influenced by chemical speciation. However, despite numerous studies over many years using a wide variety of techniques, identification of the chemical species present in

synthetic Bayer liquors, beyond the major components Na^+ , OH^- , $\text{Al}(\text{OH})_4^-$, and H_2O , has remained elusive. Many species have been suggested, but most have not withstood serious scrutiny.^{1–3}

Dielectric relaxation spectroscopy (DRS) probes the interaction of an electromagnetic wave of frequency ν with the sample. For an electrolyte solution of conductivity κ , DRS determines the relative dielectric permittivity, $\epsilon'(\nu)$, and the total loss, $\eta''(\nu)$, which is related to the dielectric loss $\epsilon''(\nu)$ as

$$\eta''(\nu) = \epsilon''(\nu) + \kappa/(2\pi\nu\epsilon_0) \quad (1)$$

where ϵ_0 is the permittivity of a vacuum. The complex permittivity is directly related to the fluctuations of the total

$$\hat{\epsilon}(\nu) = \epsilon'(\nu) - i\epsilon''(\nu) \quad (2)$$

dipole moment of the sample, $\vec{M}(t) = \sum \vec{\mu}_j$, which arise from the motions and interactions of the individual molecular dipole moments, $\vec{\mu}_j$.^{4,5}

Because of the long-range nature of dipole–dipole and ion–dipole interactions, DRS can be used to gain information on

* To whom correspondence should be addressed. E-mail: Richard.Buchner@chemie.uni-regensburg.de. E-mail: hefter@chem.murdoch.edu.au.

† Permanent address: Institut für Physikalische und Theoretische Chemie, Universität, Regensburg, D-93040 Regensburg, Germany.

‡ Present address: Department of Inorganic and Analytical Chemistry, University of Szeged, PO Box 440, H-6701 Szeged, Hungary.

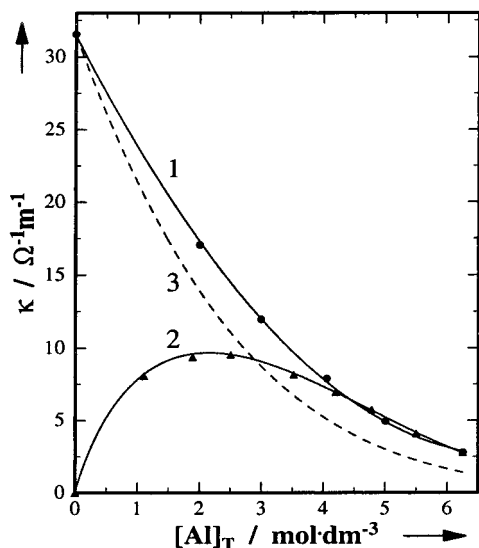


Figure 1. Effective conductivity, κ , of alkaline aluminate solutions obtained from η'' as a function of total aluminum concentration, $[\text{Al}]_{\text{T}}$, at 25 °C; curve 1 at $[\text{Na}]_{\text{T}} = 8.33 \pm 0.05 \text{ mol dm}^{-3}$, curve 2 at $[\text{Al}]_{\text{T}}/[\text{Na}]_{\text{T}} = 0.750$. Curve 3 gives the Walden-rule estimate of κ for $[\text{Na}]_{\text{T}} = 8.33 \text{ mol dm}^{-3}$.

the structure of, and the dynamics of cooperative motions in, electrolyte solutions.^{6,7} One particularly useful feature of DRS for the investigation of electrolyte solutions is that the ions themselves do not normally contribute to $\hat{\epsilon}(\nu)$, whereas (dipolar) ion pairs do. Under favorable circumstances, DRS is able not only to distinguish between the various types of ion pairs (contact, solvent-shared, and solvent-separated) but also to characterize their stabilities and dynamics.

On the other hand, the measurement of dielectric spectra for concentrated electrolyte solutions is problematic because the desired dielectric response is swamped by the conductivity contribution, $\kappa/(2\pi\nu\epsilon_0)$, especially at low frequencies (see eqs 1 and 2). This effect places severe limits on the accessible electrolyte concentration range. For example, previous DRS measurements on alkaline aluminate solutions⁸ were limited to $[\text{NaOH}]_{\text{T}} \leq 1 \text{ mol dm}^{-3}$ and $[\text{Al}]_{\text{T}} \leq 0.6 \text{ mol dm}^{-3}$, where the subscript T denotes the total or analytical concentration. However, because of the rapid increase of viscosity⁹ and consequent decrease in the conductivity (Figure 1), DRS measurements again become possible over a restricted range of higher aluminate concentrations. Accordingly, this paper presents a detailed DRS investigation of two series of concentrated alkaline aluminate solutions over the frequency range ca. 0.5–20 GHz.

2. Experimental Section

The dielectric permittivity, $\epsilon'(\nu)$, and total loss, $\eta''(\nu)$, spectra were recorded in the frequency range $\nu_{\text{min}} \leq \nu \leq 20 \text{ GHz}$ at $(25.00 \pm 0.02) \text{ °C}$ with a HP 85070M Dielectric Probe System based on a vector network analyzer (VNA). The instrument was calibrated with air, mercury, and dimethyl sulfoxide (DMSO, Ajax Chemicals, Australia, analytical grade, dried over 3 Å molecular sieve) as described in ref 10. DMSO was chosen as the third reference because its static (relative) permittivity, $\epsilon(\text{DMSO}) = 46.55$, matches the permittivity range covered by the samples, $37.7 \leq \epsilon \leq 66.1$, thus allowing an accuracy of 2% in ϵ' and η'' , relative to the static permittivity of the sample, to be obtained. In the frequency range of the VNA, the dielectric spectrum of DMSO can be described by a Cole–Cole equation with a relaxation time $\tau = 18.5 \text{ ps}$, distribution parameter $\alpha = 0.022$, and an “infinite frequency” permittivity $\epsilon_{\infty} = 5.24$ at 25

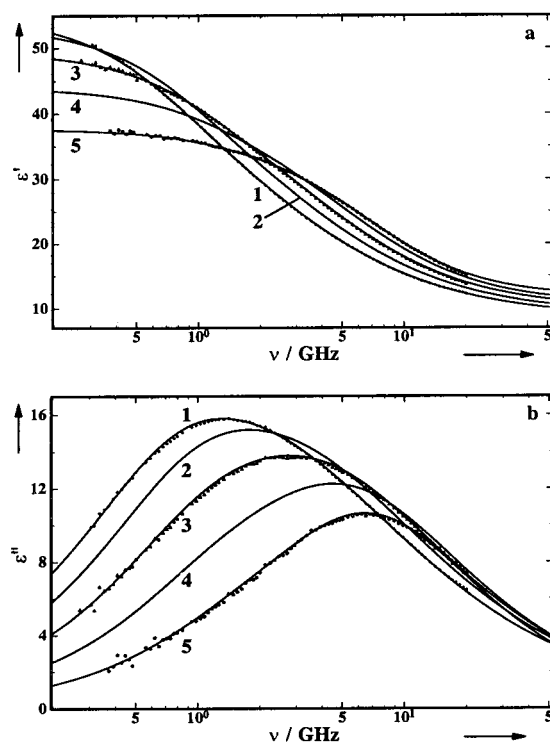


Figure 2. Dielectric dispersion, $\epsilon'(\nu)$ (a), and loss, $\epsilon''(\nu)$ (b), spectra of alkaline aluminate solutions at $[\text{Na}]_{\text{T}} = (8.33 \pm 0.05) \text{ mol dm}^{-3}$ and 25 °C. Experimental data (symbols) and the superposition of a low-frequency Debye process with a Cole–Cole equation (lines) for $[\text{Al}]_{\text{T}}/(\text{mol dm}^{-3}) = 2.00$ (5), 2.99 (4), 4.06 (3), 5.01 (2), and 6.25 (1).

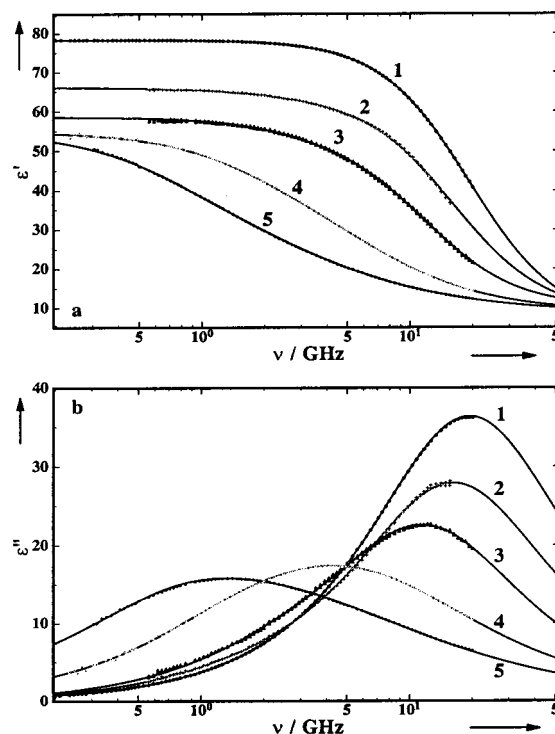


Figure 3. Dielectric dispersion, $\epsilon'(\nu)$ (a), and loss, $\epsilon''(\nu)$ (b), spectra of alkaline aluminate solutions at $[\text{Al}]_{\text{T}}/[\text{Na}]_{\text{T}} = 0.750$ and 25 °C. Experimental data (symbols) and the superposition of a low-frequency Debye process with a Cole–Cole equation (lines) for $[\text{Al}]_{\text{T}}/(\text{mol dm}^{-3}) = 0.0$ (1), 1.11 (2), 2.51 (3), 4.78 (4), and 6.25 (5).

°C.¹¹ The lowest accessible frequency, ν_{min} , depended on the conductivity of the sample and ranged from $\nu_{\text{min}} = 0.2$ –0.7 GHz, see Figures 2 and 3.

TABLE 1: Concentrations of Aluminum, [Al]_T, and Sodium, [Na]_T, Density, ρ, Viscosity, η, Effective Conductivity, κ, of Aluminate Solutions in Aqueous NaOH for [Na]_T = (8.33 ± 0.05) mol dm⁻³ at 25 °C, Together with the Parameters ε, τ₁, ε₂, τ₂, α₂, and ε_∞ of eq 3 and the Variance of the Fit, s^{2a}

[Al] _T	[Na] _T	[Al] _T /[Na] _T	ρ	η	κ	ε	τ ₁	ε ₂	τ ₂	α ₂	ε _∞	s ²
2.003	8.318	0.2409	1.339	12.66	17.06	37.71	117	35.14	23.2	0.093	11.64	0.018
2.995	8.290	0.3612	1.366	17.46	11.97	44.17	132	39.28	29.8	0.167	10.26	0.016
4.056	8.410	0.4823	1.401	25.87	7.89	49.86	149	42.10	39.4	0.215	9.46	0.016
5.005	8.364	0.5984	1.427	42.5*	4.94	54.12	173	43.50	50.0	0.252	8.62	0.010
6.253	8.290	0.7542	1.461	65*	2.79	56.05	209	44.93	65.5	0.277	8.05	0.007

^a Units: [Al]_T and [Na]_T in mol dm⁻³; ρ in kg dm⁻³; η in 10⁻³ Pa s (* extrapolated); κ in Ω⁻¹ m⁻¹; τ₁ and τ₂ in 10⁻¹² s.

TABLE 2: Concentrations of Aluminum, [Al]_T, and Sodium, [Na]_T, Density, ρ, Effective Conductivity, κ, of Aluminate Solutions in Aqueous NaOH for [Al]_T/[Na]_T = 0.750 at 25 °C, Together with the Parameters ε, τ₁, ε₂, τ₂, α₂, and ε_∞ of Eq 3 and the Variance of the Fit, s^{2a}

[Al] _T	[Na] _T	[Al] _T /[Na] _T	ρ	κ	ε	τ ₁	ε ₂	τ ₂	α ₂	ε _∞	s ²
0 ^b	0		0.99705	0			78.37	8.27	0	5.6	
1.106	1.466	0.7542	1.092	8.07	66.11	88.4	63.71	9.75	0.0	8.47	0.035
1.888	2.505	0.7537	1.155	9.73	61.07	72.9	58.00	11.9	0.0	9.98	0.039
2.505	3.321	0.7542	1.202	9.54	58.63	66.1	53.94	13.3	0.011	9.90	0.042
2.776	3.681	0.7542	1.222	9.42	57.33	88.7	54.21	14.8	0.052	8.71	0.036
3.522	4.697	0.7498	1.277	8.15	55.67	67.5	49.07	17.9	0.069	8.98	0.013
4.200	5.601	0.7498	1.325	6.94	55.03	79.9	47.26	22.8	0.120	8.43	0.032
4.780	6.347	0.7498	1.364	5.73	55.11	102	46.22	28.5	0.153	8.50	0.014
5.499	7.334	0.7498	1.413	4.09	56.66	147	46.35	42.4	0.218	8.14	0.011
6.253	8.290	0.7542	1.461	2.79	56.05	209	44.93	65.5	0.277	8.05	0.007

^a Units: [Al]_T and [Na]_T in mol dm⁻³; ρ in kg dm⁻³; κ in Ω⁻¹ m⁻¹; τ₁, τ₂ in 10⁻¹² s. ^b Reference 10.

Two series of solutions were investigated. The first covered aluminum concentrations $2.00 \leq [\text{Al}]_{\text{T}}/\text{mol dm}^{-3} \leq 6.25$ at a constant sodium concentration of $[\text{Na}]_{\text{T}} = 8.33 \pm 0.05 \text{ mol dm}^{-3}$. This series corresponds to the replacement, at constant formal (stoichiometric) ionic strength I , of OH^- by “ $\text{Al}(\text{OH})_4^-$ ” and will be referred to throughout as the “constant I ” series. The second series covered a similar range of $[\text{Al}]_{\text{T}}$ but at a constant ratio of $[\text{Al}]_{\text{T}}/[\text{Na}]_{\text{T}} = 0.750 \pm 0.005$. This series corresponds, in essence, to the replacement of solvent water by solute electrolyte ($\text{NaOH} + \text{“NaAl}(\text{OH})_4\text{”}$) and will be referred to as the “constant $\text{Al}_{\text{T}}/\text{Na}_{\text{T}}$ ” series. This ratio is related (but is not numerically equivalent) to the “A/C” (alumina to caustic) ratio employed industrially. It should also be noted that “ $\text{NaAl}(\text{OH})_4^-$ ” will be used as a convenient shorthand for all the aluminum-containing species present in alkaline aluminate solutions.

Solutions were prepared in volumetric flasks by diluting a stock solution made from analytical grade NaOH and Al (Ajax) with water or 8.3 mol dm^{-3} NaOH. As some of the solutions under study were supersaturated, all solutions contained 200 ppm Na-gluconate, which is below the limit of detection by DRS, as a seed poison. For each concentration, at least two spectra were recorded using independent calibration runs, either with the same sample or, if precipitation was observed, using solutions prepared immediately before the experiment. It should be noted that the freshly prepared concentrated liquors slowly degassed, which also affected the reproducibility of the spectra. For example, the 2.77 mol dm^{-3} solution of Table 2 was clearly an outlier from the data as a whole (see Figures 6 and 7).

3. Data Analysis

Each spectrum was analyzed separately to determine the slightly calibration-dependent effective conductivity, κ , at each concentration. As previously,⁸ the conductivity was obtained by fitting the experimental total loss curve to eq 1. The κ values obtained are broadly consistent (Figure 1) with those estimated from Walden’s rule using literature data^{12,13} for the conductivities and transport numbers of Na^+ and OH^- and our previous estimates⁸ for $\text{Al}(\text{OH})_4^-$.

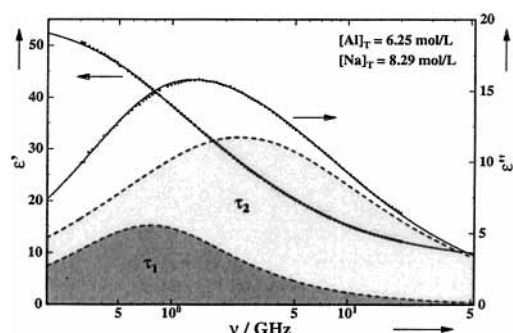


Figure 4. Dielectric dispersion, $\epsilon'(\nu)$, and loss, $\epsilon''(\nu)$, spectrum of an alkaline aluminate solution with $[\text{Al}]_{\text{T}} = 6.25 \text{ mol dm}^{-3}$ in aqueous NaOH at $[\text{Al}]_{\text{T}}/[\text{Na}]_{\text{T}} = 0.750$ and 25 °C. Experimental data (symbols) and superposition of a low-frequency Debye process with a Cole–Cole equation (lines). Shaded areas indicate the contributions of processes 1 and 2 to $\epsilon''(\nu)$.

After correction of η'' for the Ohmic loss, $\kappa/(2\pi\nu\epsilon_0)$, the individual complex permittivity spectra were combined, providing sufficient reproducibility was obtained ($\pm 2\%$), and fitted to various conceivable relaxation models. For all of the electrolyte solutions studied, it was found that $\hat{\epsilon}(\nu)$ was best fitted by the superposition of a lower-frequency Debye process with a dominating higher-frequency process having a Cole–Cole distribution of relaxation times (see Figure 4). This situation is expressed as

$$\hat{\epsilon}(\nu) = \frac{\epsilon - \epsilon_2}{1 + i2\pi\nu\tau_1} + \frac{\epsilon_2 - \epsilon_\infty}{1 + (i2\pi\nu\tau_2)^{1-\alpha_2}} + \epsilon_\infty \quad (3)$$

with “static” permittivity ϵ , “infinite frequency” permittivity $\epsilon_\infty = \lim_{\nu \rightarrow \infty} \epsilon'$, relaxation times τ_1 and τ_2 , and relaxation-time distribution parameter $0 \leq \alpha_2 < 1$. The amplitudes (relaxation strengths) of processes 1 and 2 are defined as $S_1 = \epsilon - \epsilon_2$ and $S_2 = \epsilon_2 - \epsilon_\infty$, where ϵ_2 is the low-frequency limit of the second dispersion step. Other conceivable relaxation models, like a single Cole–Davidson equation with an asymmetric distribution of relaxation times, exhibit systematic deviations between the

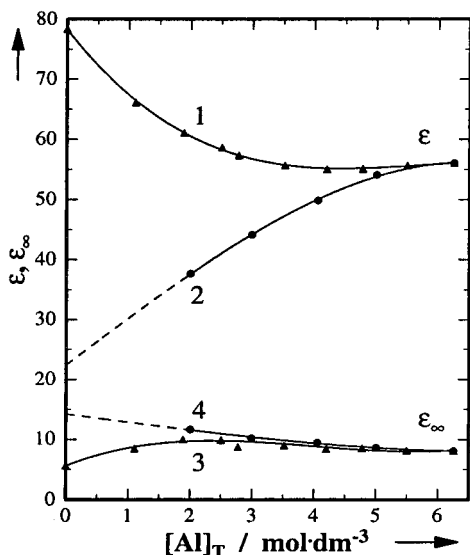


Figure 5. Static permittivity, ϵ (curves 1 and 2), and “infinite frequency” permittivity, ϵ_∞ (curves 3 and 4), of alkaline aluminate solutions as a function of $[\text{Al}]_T$ at 25 °C. Curves 1 and 3 at $[\text{Al}]_T/[\text{Na}]_T = 0.750$; curves 2 and 4 at $[\text{Na}]_T = 8.33 \pm 0.05 \text{ mol dm}^{-3}$.

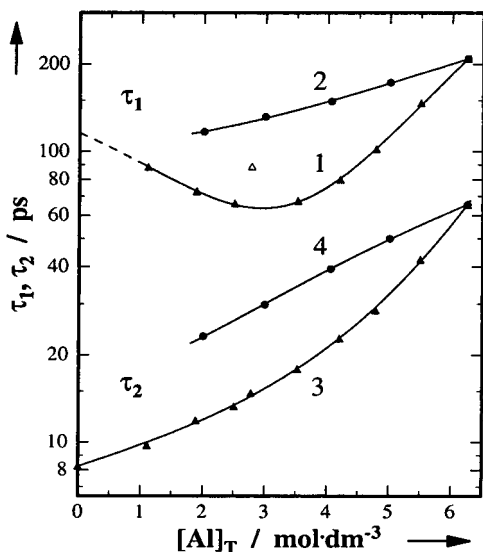


Figure 6. Dielectric relaxation times associated with the solute, τ_1 (curves 1 and 2), and the solvent, τ_2 (curves 3 and 4), of alkaline aluminate solutions as a function of $[\text{Al}]_T$ at 25 °C. Curves 1 and 3 at $[\text{Al}]_T/[\text{Na}]_T = 0.750$; curves 2 and 4 at $[\text{Na}]_T = 8.33 \pm 0.05 \text{ mol dm}^{-3}$ (open symbol point not considered in the analysis).

experimental data and the fitted $\hat{\epsilon}(\nu)$. The relaxation parameters obtained for the present model are summarized in Tables 1 (constant I series) and 2 (constant $[\text{Al}]_T/[\text{Na}]_T$ series) together with the variance of the fit, s^2 , the effective conductivity, κ , and (where available) the density, ρ , and the viscosity, η of the solutions.

4. Results and Discussion

4.1. General Comments. The DR spectra for the two series are summarized in Figures 2 and 3. At constant $[\text{Al}]_T/[\text{Na}]_T$, as water is replaced by both NaOH and “ $\text{NaAl}(\text{OH})_4$ ”, there is a marked decrease in the permittivity of the solutions, along with a dramatic broadening and shift to lower frequencies of the loss peak (Figures 3 and 5). These effects can be explained in terms of the emergence of a lower frequency process centered on 0.8 GHz and a concomitant decrease in the higher frequency process

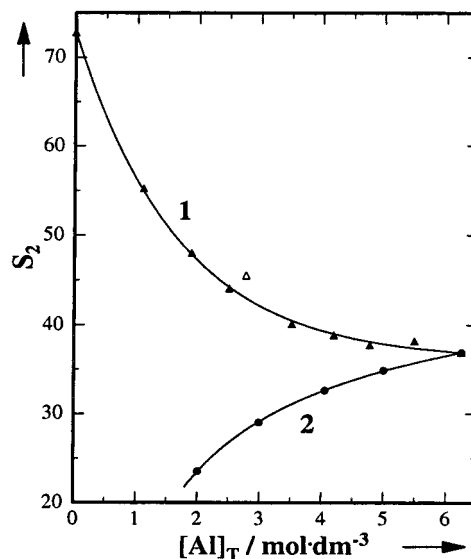


Figure 7. Dispersion amplitude, S_2 , of the solvent relaxation process of alkaline aluminate solutions as a function of $[\text{Al}]_T$ at 25 °C. Curve 1 at $[\text{Al}]_T/[\text{Na}]_T = 0.750$; curve 2 at $[\text{Na}]_T = 8.33 \pm 0.05 \text{ mol dm}^{-3}$ (open symbol point not considered in the analysis).

(Figure 4). For the constant I series, there is an increase in permittivity and a broadening and shift to lower frequencies of the loss spectrum (Figures 2 and 5).

A further feature of the DR spectra is the unusually high values of ϵ_∞ (Figure 5). Although there is some uncertainty in this quantity because the spectra were limited to $\nu \leq 20 \text{ GHz}$, the present values are significantly greater than those found for pure water and typical electrolyte solutions ($\epsilon_\infty \approx 5$).^{14–16} These large ϵ_∞ values suggest an increasing contribution to the relaxation process in the far IR region. This could be due to increasing numbers of freely rotating water molecules in these concentrated electrolyte solutions (which seems highly unlikely) or, more plausibly, to an increase in fast proton transfer ($\text{H}_2\text{O} \rightarrow \text{OH}^-$). A similar effect (but involving $\text{H}_3\text{O}^+ \rightarrow \text{H}_2\text{O}$ proton transfer) was reported by Zoidis et al.¹⁷ for concentrated HCl(aq) solutions. For the constant $[\text{Al}]_T/[\text{Na}]_T$ series, ϵ_∞ increased with increasing solute concentration, reaching a plateau of $\epsilon_\infty \approx 9$ at $[\text{Al}]_T \approx 2 \text{ mol dm}^{-3}$ (Figure 5, curve 3). On the other hand, the replacement of OH^- by $\text{Al}(\text{OH})_4^-$ at constant I resulted in a small but steady decrease in ϵ_∞ (Figure 5, curve 4). It is noteworthy that the value of $\epsilon_\infty \approx 14$, obtained by extrapolating the constant I data to $[\text{Al}]_T = 0$ and which corresponds to a solution of $\approx 8.3 \text{ mol dm}^{-3}$ NaOH, is much higher than the values obtained in less concentrated NaOH solutions ($\epsilon_\infty(c) \approx \epsilon_\infty(\text{H}_2\text{O}) \approx 5$).⁸

4.2. Fast Relaxation Process. The higher frequency process (Figure 4) is readily assigned to (solvent) water relaxation. For the constant $[\text{Al}]_T/[\text{Na}]_T$ series, the relaxation time τ_2 increases significantly with increasing electrolyte concentration (Figure 6, curve 3), and at constant I , τ_2 increases as $\text{Al}(\text{OH})_4^-$ replaces OH^- (Figure 6, curve 4). For both series, some of this increase can be related to an increase in solution viscosity. However, at higher aluminate concentrations, solution viscosity increases much more rapidly than τ_2 , indicating that under such conditions the water relaxation process does not obey the Stokes–Einstein–Debye equation characteristic for rotational diffusion of individual molecules.^{6,19} This is consistent with the idea¹⁶ of $\tau(\text{H}_2\text{O})$ being a measure of the dwelling time of water molecules on the H-bonded network, prior to their rapid rotation with a correlation time of $\sim 0.5 \text{ ps}$. The DR spectra of both $\text{NaCl}(\text{aq})$ ¹⁰ and $\text{NaOH}(\text{aq})$ ⁸ indicate that neither $\text{Na}^+(\text{aq})$ nor $\text{OH}^-(\text{aq})$

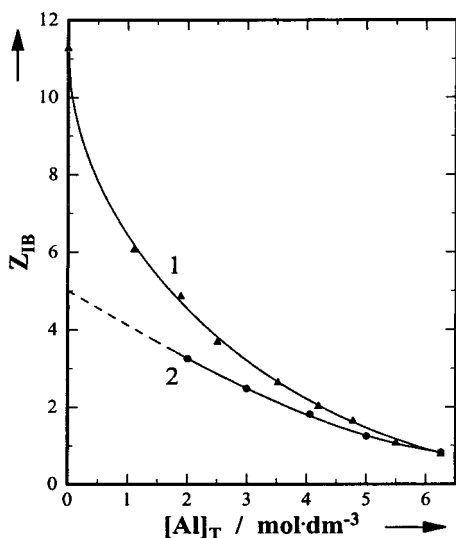


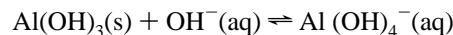
Figure 8. Effective solvation number, Z_{IB} , of alkaline aluminate solutions as a function of $[Al]_T$ at 25 °C. Curve 1 at $[Al]_T/[Na]_T = 0.750$; curve 2 at $[Na]_T = 8.33 \pm 0.05 \text{ mol dm}^{-3}$.

significantly alter $\tau(\text{H}_2\text{O})$. This suggests that it is the hydrogen-bond interactions with the aluminate species that slow the overall dynamical behavior of the water molecules in these solutions. However, from the analysis of the corresponding dispersion amplitude, see below, it emerges that these interactions are not strong enough to “freeze” the motion of the H_2O molecules in the hydration shell of $\text{Al}(\text{OH})_4^-$, in contrast to the effect of small metal ions such as Na^+ .¹⁰

The dispersion amplitude $S_2 (= \epsilon_2 - \epsilon_\infty)$ of the fast process (Figure 7) decreases monotonically with increasing electrolyte concentration at constant Al_T/Na_T but increases as $\text{Al}(\text{OH})_4^-$ replaces OH^- at constant I . The values of S_2 can be used to derive solvation numbers, Z_{IB} , via the Cavell equation, following the procedure outlined previously.¹⁰ However, as ionic conductivities required to account for the different behavior of Na^+ and OH^- ⁸ are not available for the present solutions, only the limiting case of negligible kinetic depolarization was considered. This yields an upper limit for Z_{IB} , which is a measure of the number of tightly bound (“frozen”) H_2O molecules. From the investigation of dilute NaOH and $\text{NaAl}(\text{OH})_4$ solutions,⁸ Z_{IB} may be estimated to decrease by roughly 10% by assuming that Na^+ and the aluminate species contribute under the more reasonable slip boundary conditions.

At constant I , replacement of OH^- by $\text{Al}(\text{OH})_4^-$ shows (Figure 8, curve 2) that $\text{Al}(\text{OH})_4^-$ is less strongly solvated than OH^- , consistent with our previous findings in more dilute solutions.⁸ The extrapolated value of $Z_{IB} \approx 5$ at $[Al]_T = 0$, corresponding to $\sim 8.3 \text{ mol dm}^{-3}$ NaOH is broadly consistent with the value that might be anticipated from measurements at lower concentrations of NaOH (see Figure 2 in ref 8). For the constant Al_T/Na_T series, Z_{IB} decreases markedly (Figure 8, curve 1) with increasing electrolyte concentration. Indeed, the value reached at very high concentrations ($Z_{IB} \approx 1$) is less than might be expected from the amounts of Na^+ and OH^- present, which suggests a “melting” of the hydration shells around the ions present as a result of co-sphere overlap and/or packing effects. Interestingly, the constant Al_T/Na_T series extrapolates to $Z_{IB}(c = 0) \approx 11$. This value is the same as that which can be implied from our previous measurements at lower concentrations⁸ and is consistent with the interpretation that the number of water molecules irrotationally bound to $\text{Al}(\text{OH})_4^-$ is negligible. It is interesting to note that the inequality $Z_{IB}(\text{OH}^-) \gg Z_{IB}(\text{Al}$

$(\text{OH})_4^-)$ is consistent with the well-known fact that dilution causes the equilibrium



to shift to the left.

4.3. Slow Relaxation Process. The slow process, which has a relaxation time of $\tau_1 \approx 60\text{--}200 \text{ ps}$ (Figure 6, curves 1 and 2), is reasonably assigned to a solute species. However, for reasons given below, such a species cannot be a simple $[\text{Na}^+\text{Al}(\text{OH})_4^-(\text{aq})]^0$ ion pair. Replacement of OH^- by $\text{Al}(\text{OH})_4^-$ at constant I causes a monotonic increase in τ_1 (Figure 6, curve 2). As this increase is proportional to the solution viscosity,⁹ thus ruling out a major kinetic contribution¹⁸ to τ_1 along this path, an effective rotational radius, $r_{\text{eff}} = 82 \text{ pm}$, can be derived via the Stokes–Einstein–Debye equation.^{6,19} This very small value of r_{eff} means either that the relaxing “particle” is very small or that it is of spherical or cylindrical symmetry rotating under near-slip boundary condition. Some support for the latter comes from the rather large intercept of $\tau_1(\eta = 0) \approx 100 \text{ ps}$.

The only species small enough to explain this result is OH^- . However, no such contribution is observed in the DR spectra of $\text{NaOH}(\text{aq})$,⁸ and the dispersion amplitude of the present process, $S_1 (= \epsilon - \epsilon_2)$, requires a species of much higher dipole moment. A species of spherical symmetry can also be ruled out because the only realistic candidate, the pseudotetrahedral $\text{Al}(\text{OH})_4^-$ ion, has also been shown not to make such a contribution at lower concentrations⁸ and would be expected to have a near-zero dipole moment. Of the various species of approximately cylindrical symmetry that might be present,²⁰ one possibility is the dimer $[(\text{HO})_3\text{Al}-\text{O}-\text{Al}(\text{OH})_3]^{2-}$, first proposed by Moolenaar et al.²¹ on the basis of vibrational spectroscopy. Although the evidence for this species is not as unequivocal as is often assumed,^{22,23} its existence is consistent with many observations on concentrated alkaline aluminate solutions, unlike most of the other aluminate species that have been proposed.^{24,25} However, the dipole moment estimated for the Moolenaar dimer (MD^{2-}) using the quantum mechanical calculations of Gale et al.²⁰ is far too low ($\mu \approx 1.5 \text{ D}$) to explain the dispersion amplitude S_1 . This becomes obvious from rearranging the Cavell equation²⁶ to

$$Y = \mu_e^2 \cdot c_1 \quad (4)$$

where

$$Y = \frac{2\epsilon - 1}{\epsilon} \cdot \frac{k_B T \epsilon_0}{N_A \cdot S_1} \quad (5)$$

is used to represent the experimentally determinable quantities on the RHS of eq 5. In eqs 4 and 5, c_1 is the concentration of the dipolar species causing the solute relaxation process and $\mu_e = \mu_1/(1 - \alpha_1 f_1)$ is its (unknown) effective dipole moment; μ_1 ($0.6 \mu_1 \lesssim \mu_e \lesssim \mu_1$) is the corresponding (gas-phase) dipole moment, α_1 is its polarizability, f_1 is the corresponding reaction field factor, and the other symbols have their usual meanings. The plot (Figure 9) of Y vs $[Al]_T$ reveals that $\mu_e \approx 10 \text{ D}$ is required if all of the aluminate were present as the relaxing species (the required value of μ_e would be even larger if some aluminate was present as other species such as $\text{Al}(\text{OH})_4^-$). Similar considerations seemingly rule out all other plausible oligomeric aluminate ions.²⁰

Apart from some highly complicated aluminate-containing species (for which no credible evidence exists in concentrated alkaline solutions), the only plausible species remaining to

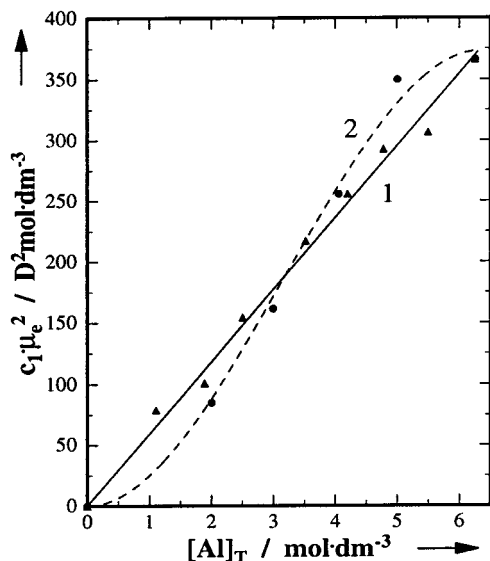


Figure 9. Scaled amplitude, $Y = c_1\mu_e^2$, of the solute relaxation process of alkaline aluminate solutions as a function of $[\text{Al}]_T$ at 25 °C. Curve 1 at $[\text{Al}]_T/[\text{Na}]_T = 0.750$; curve 2 at $[\text{Na}]_T = 8.33 \pm 0.05 \text{ mol dm}^{-3}$.

account for the present solute-related relaxation process are sodium/aluminate ion pairs. As noted above, the simplest of these species, $[\text{Na}^+\text{Al}(\text{OH})_4^-(\text{aq})]^0$, is ruled out because previous measurements at lower concentrations have shown that the lifetime of such a species, which almost certainly exists in these solutions,²⁴ is too short to be detected on the DRS time scale.⁸

The next most obvious choice is a $\text{Na}^+-\text{MD}^{2-}(\text{aq})$ ion pair. A contact ion pair seems unlikely both from solution X-ray measurements²⁴ and from detailed Raman studies.²⁵ If the ion pair is assumed to be solvent-shared (SIP) and to rotate approximately around the Al–Al axis, a dipole moment of $\sim 32 \text{ D}$ is estimated from the charge separation in the ion pair. Combination of this value with the Cavell equation (eq 4) produces reasonable concentrations ($0 \leq c_1/\text{mol dm}^{-3} \leq 0.35$) proportional to Y for this species for both the constant I and constant $[\text{Al}]_T/[\text{Na}]_T$ series of measurements. In other words, a maximum of approximately 5–6% of the aluminum would be in the form of $\text{Na}^+-\text{MD}^{2-}(\text{aq})$ SIP.

It is also possible that the $\text{Na}^+-\text{MD}^{2-}(\text{aq})$ ion pair is of the double solvent separated (2SIP) type. Although the low hydration numbers (Figure 8) indicate this is improbable, the data are insufficient to make the distinction. The only remaining possibilities would seem to be Na^+ ion pairs with aluminate species more complex than $\text{MD}^{2-}(\text{aq})$ or some type of cooperative interaction between the very closely packed ions and solvent molecules. The present data would be consistent with such species or process but neither confirm nor disprove their existence, although large-scale cooperative interactions seem unlikely for the more dilute solutions in the $[\text{Al}]_T/[\text{Na}]_T$ series. Note also, that for this series, τ_1 goes through a minimum at $[\text{Al}]_T \approx 3 \text{ mol dm}^{-3}$ (Figure 6, curve 1). As the solution viscosity increases monotonically under such conditions, this behavior suggests a kinetic contribution to the slow relaxation process at lower concentrations, which is common for ion pairs.¹⁸

4.4. Concluding Remarks. As has proven to be the case for many detailed investigations of concentrated alkaline aluminate solutions employing a wide variety of techniques,^{1–3,20,22–24}

unequivocal evidence of the species present remains elusive. The most straightforward explanation of the present DRS data is that the slow relaxation process detected is associated with a $\text{Na}^+-\text{MD}^{2-}(\text{aq})$ SIP, but it must be emphasized that more complex explanations cannot be ruled out. Regardless of its exact nature, the species causing the low-frequency relaxation must be added to the list of obvious (Na^+ , OH^- , $\text{Al}(\text{OH})_4^-$, $\text{NaOH}(\text{aq})$, and $\text{NaAl}(\text{OH})_4(\text{aq})$ ion pairs) and highly probable (MD^{2-}) species that exist in concentrated alkaline sodium aluminate solutions.

Acknowledgment. The authors thank A.L.Rohl for providing the dipole moments of the dimeric aluminate species of Ref 20. This work was funded by the Australian Research Council and the Australian alumina industry (Alcoa World Alumina, Comalco Aluminum, Queensland Alumina and Worsley Alumina) through the Australian Mineral Industries Research Association Project P380B. Support by the Deutsche Forschungsgemeinschaft for R.B. is gratefully acknowledged.

References and Notes

- (1) Eremin, N. I.; Volokhov, Y. A.; Mironov, V. E. *Russ. Chem. Rev.* **1974**, *43*, 92.
- (2) Zambo, J. *Light Metals* **1986**, 199.
- (3) Sipos, P.; May, P. M.; Hefter, G. T.; Kron, I. *J. Chem. Soc., Chem. Commun.* **1994**, 2355.
- (4) (a) Böttcher, C. F. J. *Theory of Electric Polarization*, 2nd ed.; Elsevier: Amsterdam, 1973; Vol. 1. (b) Böttcher, C. F. J.; Bordewijk, P. *Theory of Electric Polarization*, 2nd ed.; Elsevier: Amsterdam, 1978; Vol. 2.
- (5) Scaife, B. K. P. *Principles of Dielectrics*; Clarendon: Oxford, U.K., 1989.
- (6) Barthel, J.; Buchner, R.; Eberspächer, P.-N.; Münsterer, M.; Stauber, J.; Wurm, B. *J. Mol. Liq.* **1998**, *78*, 82.
- (7) Buchner, R.; Barthel, J. *Annu. Rep. Prog. Chem. C* **2001**, *97*, 349.
- (8) Buchner, R.; Hefter, G. T.; May, P. M.; Sipos, P. *J. Phys. Chem. B* **1999**, *103*, 11186.
- (9) Sipos, P.; Stanley, A.; Bevis, S.; Hefter, G. T.; May, P. M. *J. Chem. Eng. Data* **2001**, *46*, 657.
- (10) Buchner, R.; Hefter, G. T.; May, P. M. *J. Phys. Chem. A* **1999**, *103*, 1.
- (11) Barthel, J.; Buchner, R.; Münsterer, M. Unpublished results.
- (12) DeWayne, H. J.; Hamer, W. J. *Sci. Technol. Aerosol. Rep.* **1969**, *7*, 28.
- (13) Troshin, V. P.; Zvyagina, E. V. *Sov. Electrochem. Engl. Trans.* **1972**, *8*, 1669.
- (14) Barthel, J.; Buchner, R.; Münsterer, M. In *Electrolyte Data Collection, Part 2: Dielectric Properties of Water and Aqueous Electrolyte Solutions*; Kreysa, G., Ed.; Chemistry Data Series; DECHEMA: Frankfurt, Germany, 1995; Vol. XII.
- (15) Kaatz, U. *J. Solution Chem.* **1997**, *26*, 1049.
- (16) Buchner, R.; Barthel, J.; Stauber, J. *Chem. Phys. Lett.* **1999**, *306*, 57.
- (17) Zoidis, E.; Yarwood, J.; Besnard, M. *J. Phys. Chem. A* **1999**, *103*, 220.
- (18) Buchner, R.; Barthel, J. *J. Mol. Liq.* **1995**, *63*, 55.
- (19) Dote, J. L.; Kivelson, D.; Schwartz, R. N. *J. Phys. Chem.* **1981**, *85*, 2169.
- (20) Gale, J. D.; Rohl, A. L.; Watling, H. R.; Parkinson, G. M. *J. Phys. Chem. B* **1998**, *102*, 10372.
- (21) Moolenaar, R. J.; Evans, J. C.; McKeever, L. D. *J. Phys. Chem.* **1970**, *74*, 3629.
- (22) Watling, H.; Sipos, P.; Byrne, L.; Hefter, G. T.; May, P. *Appl. Spectrosc.* **1999**, *55*, 415.
- (23) Sipos, P.; Capewell, S. G.; May, P. M.; Hefter, G. T.; Laurency, G.; Lukács, F.; Roulet, R. *J. Chem. Soc., Dalton Trans.* **1998**, 3007.
- (24) Radnai, T.; May, P. M.; Hefter, G. T.; Sipos, P. *J. Phys. Chem. A* **1998**, *102*, 7841.
- (25) Sipos, P.; May, P. M.; Hefter, G. T. Unpublished observations.
- (26) Cavell, E. A. S.; Knight, P. C.; Sheikh, M. A. *J. Chem. Soc., Faraday Trans.* **1971**, *67*, 2225.